

UC Irvine

UC Irvine Previously Published Works

Title

Substrate-binding to lactate dehydrogenase perturbs an intersubunit equilibrium sensed by engineered tryptophan-248

Permalink

<https://escholarship.org/uc/item/6x21b74x>

Journal

Biochemical Society Transactions, 15(6)

ISSN

0300-5127

Authors

WALDMAN, ADAM DB
BARSTOW, DAVID A
CLARKE, ANTHONY A
[et al.](#)

Publication Date

1987-12-01

DOI

10.1042/bst0151158

Copyright Information

This work is made available under the terms of a Creative Commons Attribution License, available at <https://creativecommons.org/licenses/by/4.0/>

Peer reviewed

Substrate-binding to lactate dehydrogenase perturbs an intersubunit equilibrium sensed by engineered tryptophan-248

ADAM D. B. WALDMAN*, DAVID A. BARSTOW†, ANTHONY A. CLARKE*, ENRICO GRATTON‡, TONY ATKINSON† and J. JOHN HOLBROOK*

*Department of Biochemistry, University of Bristol Medical School, Bristol BS8 1TD, U.K.; †P.H.L.S. Centre for Applied Microbiology and Research, Microbial Technology Laboratory, Salisbury SP4 0JG, U.K., and ‡Department of Physics, 1110 West Green Street, Urbana, IL 61801, U.S.A.

The time-resolved fluorescence properties of tryptophan residues in proteins are very sensitive to small changes in local environment (Beechem & Brand, 1985). However, this potentially useful optical probe of protein internal mobility has not been widely used because most proteins have multiple tryptophan residues (average 3.6) with overlapping spectral bands. To circumvent this ambiguity the techniques of molecular genetics were used to construct a lactate dehydrogenase gene which lacks tryptophan codons (Waldman *et al.*, 1987), and site-directed mutagenesis of this gene was used to reintroduce a single tryptophan at a specific site within the known primary and three-dimensional structure at which information on environment changes is sought. The method has revealed domain re-arrangements in the 0.1 ms timescale during recognition of the substrate pyruvate and the allosteric effector fructose 1,6-bisphosphate (Atkinson *et al.*, 1987), and has partly characterized stable intermediates during the re-folding of this protein from guanidinium hydrochloride (Clarke *et al.*, 1987).

Molecular recognition depends upon fast internal motions in proteins and we report here the nanosecond properties of a single-tryptophan construct based on *Bacillus stearothermophilus* lactate dehydrogenase, in which wild-type tyrosine-248 is replaced by tryptophan (and the three natural tryptophans at 80, 150 and 203 by tyrosine). The 248-substitution was directed by the mismatch of a 23mer oligonucleotide to the whole gene between the *Hind*III and *Pst*I sites, the mutant protein over-produced by pLDH41 in *Escherichia coli* TG2 cells and purified by affinity chromatography on oxamate-Agarose from pLDH41 in exactly the same manner as for other mutants (Clarke *et al.*, 1986). The 248-site is normally tryptophan in other lactate dehydrogenases and is well placed to sense structural re-arrangements: being (1) close to the very stable *Q*-axis intersubunit contact and (2) just two residues away from isoleucine-250 which forms the hydrophobic surface which is tightly covered when the dihydropyridine ring of NADH binds in the active centre.

Fig. 1 shows the modulation ratios and phase differences of the fluorescence of single-tryptophan-248 dehydrogenase measured with the multi-frequency phase fluorometer described by Alcalá *et al.* (1987). In the apo-tetrameric protein (stabilized by fructose 1,6-bisphosphate) the single tryptophan fluorescence is analysed as two logarithmic decays (82% 5.0 ns, 18% 1.4 ns) and in the very stable quaternary complex formed between the protein, regulator, NAD⁺ and oxalate, the proportions are reversed (21% 4.8 ns, 79% 0.61 ns). This frequency-domain result has been

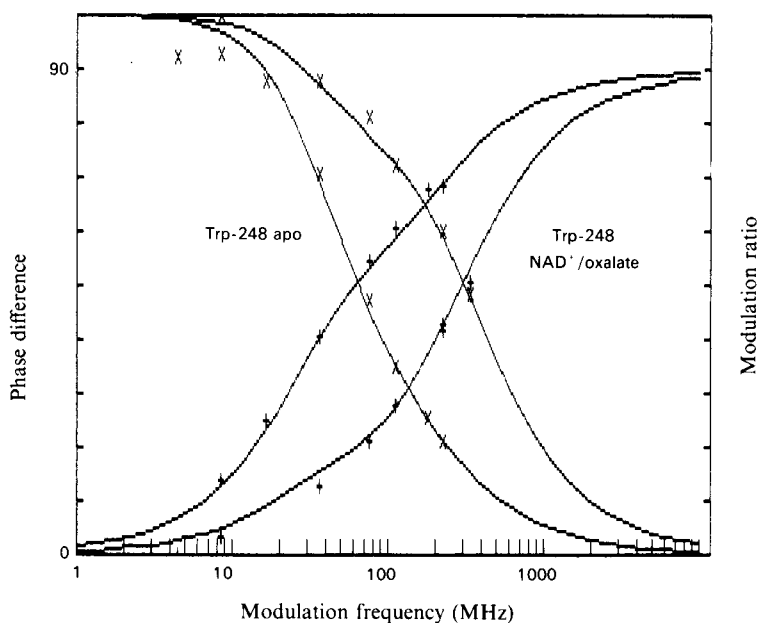


Fig. 1. Frequency-domain measurements of fluorescence lifetimes of single-tryptophan-248 *B. stearothermophilus* lactate dehydrogenase

Measured phase difference (+) and modulation ratio (x) of 10 μ M-enzyme solution in 0.1 M-triethanolamine HCl buffer, pH 6 and 10 mM-fructose 1,6-bisphosphate at 25°C as a function of modulation frequency is compared to the predicted continuous curves calculated from the lifetime and pre-exponential factors given in the text. The results and pair of curves at the higher frequencies are from a solution containing in addition 0.1 mM-NAD⁺ and 1 mM-Na oxalate.

quantitatively confirmed by time-domain measurements which also revealed, in the apo-enzyme, a logarithmic decay of 248-fluorescence anisotropy from $r_0 = 0.188$ to $r_\infty = 0.056$ with $\tau_c = 4.1$ ns (see Clarke *et al.*, 1987, for instrument detail of the same experiment on tryptophan-203 enzyme). r_0 and r_∞ are the fluorescence anisotropies at time zero and a long time compared to τ_c , the rotational correlation time for the anisotropy decay. The increase in proportion of short lifetimes is consistent with the quench to 34% of the equilibrium tryptophan fluorescence when the quaternary complex forms.

Direct interaction of the coenzyme ring with residue-248 is not sterically possible, and extensive absorbance measurements failed to reveal a chromophore at 300–400 nm as a possible acceptor of resonance energy. We thus conclude that formation of a quaternary complex analogue induces structural rearrangements which extend not only to the coenzyme-loop domain but also up to, and possibly across, the solvent end of helix-3G at the intersubunit Q -axis. The two-state model of Alcalá *et al.* (1987) and the fast fluorescence anisotropy correlation time of 4 ns predict the shorter component may arise from an environment with a lifetime

much shorter than the 600 ps – 1.1 ns decay actually measured – and that the longer lifetime may be greater than the measured 4 ns. Measurements on a construct prepared by re-folding the mono-tryptophan subunit with a large excess of tryptophanless subunits will test whether the structural rearrangement is transmitted not only up to, but across the Q -axis interface.

- Alcalá, J. R., Gratton, E. & Prendergast, F. G. (1987) *Biophys. J.* **51**, 697–604
 Atkinson, T., Barstow, D. A., Chia, W. N., Clarke, A. R., Hart, K. W., Waldman, A. D. B., Wigley, D. B., Wilks, H. M. & Holbrook, J. J. (1987) *Biochem. Soc. Trans.* **15**, 991–993
 Beechem, J. & Brand, L. (1985) *Annu. Rev. Biochem.* **54**, 43–71
 Clarke, A. R., Wigley, D. R., Barstow, D. A., Atkinson, T., Chia, W. N. & Holbrook, J. J. (1986) *Nature (London)* **324**, 699–702
 Clarke, A. R., Barstow, D. A., Atkinson, T., Waldman, A. D. B., Wilks, H. M., Hart, K. W., Birch, D. J. S., Chia, W. N. & Holbrook, J. J. (1987) *Biochem. Soc. Trans.* **15**, 1147–1148
 Waldman, A. D. B., Clarke, A. R., Wigley, D. B., Hart, K. W., Chia, W. N., Barstow, D. A., Atkinson, T., Munro, I. & Holbrook, J. J. (1987) *Biochim. Biophys. Acta* **913**, 66–71.

Received 18 June 1987

Quantitative autoradiography of delta opioid receptors in rodent brain using [³H]D-Pen²-D-Pen⁵-enkephalin as the radioligand

N. A. SHARIF, R. G. HILL and J. HUGHES

Parke-Davis Research Unit, Addenbrookes Hospital Site, Cambridge, CB2 2QB U.K.

The presence of mu, kappa and delta opioid receptors in the mammalian central nervous system (CNS) is now well documented (see Paterson *et al.*, 1983, for review). Although delta receptors have been radiolabelled in the past using [³H]D-Ala²-D-Leu⁵-enkephalin ([³H]DADLE) (see Wamsley, 1983, for review) this probe has considerable cross-reactivity with mu receptors. Recently, a conformationally restricted enkephalin analogue [³H]D-Pen²-D-Pen⁵-enkephalin ([³H]DPDPE) (Mosberg *et al.*, 1983) has been synthesized and found to be highly selective for the delta receptor. We have characterized the receptor-binding properties of this radioligand using homogenate-based assays and have subsequently determined the regional distribution of delta receptors in the guinea-pig and rat CNS using quantitative autoradiographic techniques (Sharif *et al.*, 1986).

[³H]DPDPE bound with high affinity [dissociation constant, $K_d = 5.1 \pm 0.3$ nM (5)] and to a high apparent density of delta binding sites ($B_{max} = 4.4 \pm 1.5$ pmol/mg wet wt.) in guinea-pig forebrain homogenates suspended in 50 mM-Tris/HCl (pH 7.4; containing 5 mM-MgCl₂; bovine serum albumin 2 mg/ml; bacitracin 20 µg/ml; Gulya *et al.*, 1985). Unlabelled DPDPE, DADLE, etorphine, dynorphin (1–8) and naloxone potently inhibited specific [³H]DPDPE binding in guinea-pig brain membranes with apparent inhibition constants (K_i) of (nM): 5.5 ± 0.7 (6); 2.6 ± 0.5 (4); 4.2 ± 0.4 (4); 16.4 ± 1 (4) and 16.3 ± 1.5 (4), respectively, while the respective mu- and kappa-selective ligands, D-Ala²-MePhe⁴-glyol-enkephalin (DAGO) and U50488, had k_i values of > 10 µM. The properties of [³H]DPDPE binding to rat brain membranes were similar to those of the guinea-pig brain (data not shown).

Cryostat sections (10 µm) of rat and guinea-pig brain cut at different anatomical levels were processed for delta-receptor autoradiography using [³H]DPDPE (8 nM) (90 min

incubation at 4°C followed by 5 min rinsing in ice-cold 50 mM-Tris/HCl buffer) and the resultant autoradiograms quantified by digital subtraction image analysis (Sharif *et al.*, 1986). As shown in Table 1, delta receptors were heterogeneously distributed in the CNS of both rodent

Table 1. Quantitative autoradiographic distribution of [³H]-DPDPE-labelled delta opioid receptors in rat and guinea-pig CNS

Digital subtraction autoradiography of [³H]DPDPE-labelled delta receptors was performed as described above. The data are mean \pm S.E.M. from three to five sections from two to three animals of each species. The concentration of the radioligand was 8 nM and the non-specific binding was defined with 1 µM unlabelled DADLE. Specific [³H]DPDPE binding represented 80–90% of the total binding. olf., olfactory; EP, external plexiform layer; S, gelatinosa, substantia gelatinosa; V, grey, ventral grey; ND, not determined.

Region	Specific binding (amol/mm ²)	
	Rat	Guinea-pig
Olfactory tubercle	592 \pm 22	275 \pm 11
Accessory olf. bulb	623 \pm 19	ND
Olfactory bulb (EP)	576 \pm 25	ND
Striatum	306 \pm 30	152 \pm 24
N. Accumbens	597 \pm 22	327 \pm 17
C. Cortex layers I–II	265 \pm 89	250 \pm 16
layers III–IV	204 \pm 22	121 \pm 16
layers V–VI	313 \pm 60	280 \pm 12
Stria terminalis	33 \pm 4	84 \pm 7
Amygdala	228 \pm 10	106 \pm 10
Hypothalamus	49 \pm 6	82 \pm 21
Habenula	50 \pm 8	90 \pm 10
Hippocampus (oriens)	83 \pm 3	65 \pm 5
Globus pallidus	50 \pm 13	111 \pm 12
Thalamus	31 \pm 5	162 \pm 13
Substantia nigra	32 \pm 6	18 \pm 2
Lateral geniculate bodies	30 \pm 4	116 \pm 13
Central grey	33 \pm 4	78 \pm 9
Superior colliculus	33 \pm 4	197 \pm 18
Inferior colliculus	68 \pm 8	94 \pm 8
Spinal cord S. gelatinosa	36 \pm 6	58 \pm 7
V. grey	7 \pm 1	19 \pm 5

Abbreviations used: CNS, central nervous system; DADLE, D-Ala²-D-Leu⁵-enkephalin; DAGO, D-Ala²-MePhe⁴-Glyol-enkephalin; DPDPE, D-Pen²-D-Pen⁵-enkephalin.